

## Rhythm of the Deep: A Computational-Linguistic Test of Duality of Patterning in Sperm Whale Codas

Mudit Sinha and Sanika Chavan

Independent Researchers

*Human language builds meaning in two combinatorial layers: a small inventory of meaningless units combines into a larger inventory of meaningful ones, which in turn combine into larger structures still. This layering, duality of patterning, is one of the design features long used to set language apart, and whether any non-human system shares it has been difficult to establish. Sperm whales are a natural place to look: they communicate in codas, short rhythmic bursts of clicks that they share, reuse, and recombine. Yet layered structure has been hard to confirm, because in raw audio acoustic similarity alone can imitate genuine combinatorial structure. Studying 1,483 codas from the Dominica Sperm Whale Project, we find a two-tier architecture in which, unexpectedly, the two tiers combine by different rules. At the lower tier, clicks form a coda not by their order but by which clicks are present together with their inter-click rhythm. At the upper tier, the resulting codas sequence into bouts with measurable second-order dependence, an NSB transfer-entropy lift of 0.132 bits ( $p = 0.002$ ). Across the single step from clicks to codas, identity becomes markedly more abstract: under tempo-scaling, click identity collapses to cluster ARI  $\approx 0.07$  while coda identity holds at ARI 0.43–0.52. Because the real risk is that acoustics rather than structure is doing the work, every claim is built to survive a destructive acoustic null. The keystone click-identity signal clears that gate, and survives even when the published click timings are discarded and clicks are detected from scratch off the raw waveform, so it cannot be an artifact of how clicks were placed. A rhythm-only imitation of the system, in turn, cannot reproduce the upper-tier sequential dependence; that failure is what makes the change of combinatorial substrate between tiers a genuine finding rather than an analysis choice. We claim structure, not meaning, which is precisely what isolating a single design feature demands: we exhibit the combinatorial signature of a duality-of-patterning-like architecture, one whose lower tier is rhythmic rather than segmental, and leave semantics and perception to behavioural work our data cannot reach. The apparatus behind these claims, including held-out structural tests, per-statistic nulls, cross-encoder consensus, and acoustic-null recoverability gates, is built to transfer to any setting where symbols must be discovered from audio rather than read off.*

### 1. Introduction

A central question in the computational study of language is which design features of human language are unique to it and which recur, in whole or in part, in other communication systems (Hockett 1960). Among these features, *duality of patterning*, a finite inventory of lower-level units, not themselves the communicatively salient

elements, combining into a larger inventory of higher-level units that are, is among the hardest to test outside human language, because the evidence has to be distinguished from mere acoustic similarity, rhythmic regularity, and recurrence, all of which can imitate symbolic structure. This is a structure-discovery problem of exactly the kind computational linguistics has developed tools for: vector-quantised tokenisation, compositionality and topographic-similarity metrics, information-theoretic sequence diagnostics, and held-out probing with carefully matched controls (Brighton and Kirby 2006; Lazaridou et al. 2018; Chaabouni et al. 2020; Resnick et al. 2020; Andreas 2019). Most of that toolkit was built and validated on text and on emergent codes from communication games; here we ask what it discovers when pointed at a non-human vocal system, and what additional safeguards are required to keep its verdicts honest in the presence of an acoustic confound that has no analogue in symbolic text. The substantive target is sperm whale codas; the transferable contribution is a discipline for separating combinatorial structure from acoustic artefact that applies wherever tokens are induced from continuous signals.

Sperm whales produce short stereotyped bursts of clicks called codas, which occur in turn-taking exchanges and act as social markers of vocal clan identity (Watkins and Schevill 1977; Rendell and Whitehead 2003; Gero, Whitehead, and Rendell 2016). Recent work expanded the labelled corpus and characterised codas at fine temporal resolution (Sharma et al. 2024). We use those annotations as the measurement backbone for a different question: Sharma et al. provide coda labels, click counts, and inter-click intervals, but they do not determine what rule combines clicks into codas, whether that rule is order-based or rhythm-based, or whether the rule changes again when codas sequence within bouts. We treat this as a computational phonology and field-linguistic structure-discovery problem: using acoustic representations as instruments for testing layered combinatorial structure in a non-human vocal system.

The structural question is not whether codas have been catalogued, but whether the catalogue has internal combinatorial architecture. A naive hypothesis is that codas are built from click units like human words from ordered phonemes (Hockett 1960). That hypothesis is easy to over-read from embeddings: acoustic similarity, rhythm, and recurrence can all imitate symbolic structure. Conversely, a purely rhythmic description could explain lower-tier coda identity without explaining whether codas behave as higher-level representation-level units in bout sequences.

We therefore ask a layered question. First, do codas form a recurring representation-level inventory that can serve as the upper unit of analysis? Second, at the click→coda tier, is coda identity carried by click identity, click order, rhythm, or some mixture? Third, at the coda→bout tier, do codas sequence as representation-level units, and can rhythm-only representations carry the same bout-level structure? Finally, under matched tempo-scaling, does click-level identity remain more rate-bound than coda-level identity, revealing an abstraction gradient across the click→coda step?

To keep those questions honest, we use three safeguards. (i) We use an ensemble of eight frozen audio encoder families spanning bioacoustic, general-audio, music/audio, and speech pretraining regimes: AVES (Hagiwara 2023), BEATs/OpenBEATs (Chen et al. 2023), VampNet (Garcia et al. 2023), Whisper (Radford et al. 2023), Perch (Ghani et al. 2023), HuBERT (Hsu et al. 2021), wav2vec 2.0 (Baevski et al. 2020), and an AVES2 checkpoint. Phase A uses 23 whole-coda views; the click-level suite uses 20 views; other tests use the eligible view set stated with the statistic. We report agreement rather than relying on a single embedding view. (ii) Every structural statistic carries a non-circular null or control appropriate to what it measures, evaluated under cross-validation blocked by recording covariates (Date, social unit, individual). (iii) Click-side and mixed click-to-coda diagnostics additionally pass through an acoustic-null recoverability gate:

we regenerate each finding from spectrum-matched, click-order-shuffled, envelope-noise-filled, and cross-coda click-replaced versions of the audio, and ask whether the destructive null reproduces the signal.

The resulting picture is more specific than “whale phonemes.”

- Codas form a recurring representation-level inventory with sequential dependence at the bout level.
- Clicks compose into codas not by stable order, but by which clicks are present plus their inter-click timing; the lower tier is inventory-plus-rhythm rather than an ordered segmental rule.
- Rhythm-only representations recover substantial lower-tier structure but fail on the upper-tier Phase E sequential-dependence test, including under a stronger dICI n-gram / variable-length-Markov-inspired counterfactual motivated by prior dICI patterning work (Hersh et al. 2022).
- Matched tempo-scaling reveals an abstraction gradient: encoder-derived whole-waveform click identity is strongly rate-bound, while coda identity remains substantially more stable, including under a same-arm coda check and under ICI-only matched tempo-scaling.

*Contributions.* The contribution is the evidence stack as a whole: Sharma-anchored click alignment, held-out structural tests, acoustic-null recoverability checks, matched-click-multiset controls with group-aware robustness, a full de-novo click-detection control that re-extracts encoder embeddings at envelope-detected click windows, rhythm-only and VLMM-inspired dICI counterfactuals, and a two-tier interpretation in which a rhythmic lower tier composes into a representation-level, sequential upper tier with a measurable abstraction gradient.

*Scope, and why it is a strength.* Duality of patterning is defined by a structural relation between two combinatorial tiers, not by the presence of word-like meanings; a system can exhibit it without our being able to read off what, if anything, its units denote. We therefore make claims at the level the data can bear, namely the geometry of induced token inventories and their combination rules under explicit nulls, and deliberately decline to claim semantics, perception, or behavioural use. This is the same discipline that the emergent-communication literature applies when it measures compositionality of a learned protocol without asserting that the agents “mean” anything by it (Lazaridou et al. 2018; Chaabouni et al. 2020). Treating the absence of a semantic claim as evidence that a structural finding is not about language inverts the logic of design-feature analysis: it is precisely by isolating one design feature at a time, and refusing to smuggle in the others, that the comparative study of communication systems makes falsifiable progress. The structural questions we do answer, namely what inventory exists, what rule composes its units, whether that rule changes across tiers, and whether an acoustic null can counterfeit the result, are computational-linguistics questions, and the methods that answer them are computational-linguistics methods.

## 2. Related Work

*Design features and the comparative study of communication systems.* The framework of design features (Hockett 1960) was introduced precisely to make the comparison between human language and animal communication tractable, by decomposing “language” into separable, individually testable properties. Subsequent computational work on non-

human systems has largely targeted single-tier sequential structure or vocal learning, including in birdsong, gibbon song, and bat vocalisations (Berwick et al. 2011; Sainburg et al. 2020; Clarke, Reichard, and Zuberbühler 2006; Prat et al. 2017), rather than the relation *between* tiers that duality of patterning names. We take up that relation directly, and we do so with the measurement apparatus that computational linguistics has built for emergent and learned codes: topographic similarity (Brighton and Kirby 2006), compositionality metrics (Lazaridou et al. 2018; Chaabouni et al. 2020; Resnick et al. 2020), and representation-level structural probes (Andreas 2019). The methodological gap we fill is that these metrics were validated where the token alphabet is given by construction; applying them to induced acoustic tokens requires an additional layer of controls, including per-statistic nulls, cross-encoder consensus, and acoustic-null recoverability gates, without which acoustic similarity can masquerade as combinatorial structure.

*Coda structure and clan identity.* Codas have long been catalogued and used to identify sperm-whale vocal clans (Watkins and Schevill 1977; Rendell and Whitehead 2003; Gero, Whitehead, and Rendell 2016; Hersh et al. 2022). Sharma et al. (2024) provide the annotated corpus and click-level ICI measurements that make our analysis possible; we use them to ask what rule combines clicks into codas and whether the carrier of structure changes at the coda-to-bout tier.

*Bioacoustic representation learning.* Frozen audio encoders and latent-space pipelines are increasingly used to inventory non-human vocal repertoires (Hagiwara 2023; Ghani et al. 2023; Sainburg, Thielk, and Gentner 2020; Goffinet et al. 2021). Our use is deliberately stricter: a result must hold across many independently trained encoder views and against a target-specific null, rather than being read from a single projected embedding space.

*Rhythm and sequence structure.* Prior sperm-whale work links clan identity to within-coda dICI patterning (Hersh et al. 2022). Bridge 6 is a non-parametric counterpart to that dICI-patterning tradition: with click-token multiset held fixed, it asks whether the remaining ICI pattern tracks encoder-geometry distance. More broadly, birdsong, gibbon song, and bat vocalisations show single-tier sequential structure or vocal learning (Berwick et al. 2011; Sainburg et al. 2020; Clarke, Reichard, and Zuberbühler 2006; Prat et al. 2017). Our question is complementary: whether the composition rule changes between adjacent tiers.

*Compositionality metrics and structural tests.* Our diagnostics are closest in spirit to language-evolution and emergent-communication measures, including topographic similarity (Brighton and Kirby 2006), compositionality metrics (Lazaridou et al. 2018; Chaabouni et al. 2020; Resnick et al. 2020), and representation-level tests (Andreas 2019). We adapt that tradition to non-human acoustics with blocked held-out evaluation, per-statistic nulls, cross-encoder consensus, and acoustic-null gates; the information-theoretic toolkit is standard (Nemenman, Shafee, and Bialek 2002; Schreiber 2000; Benjamini and Hochberg 1995).

### 3. Data and Methods

*Recordings and annotations.* We use audio from the Dominica Sperm Whale Project at 16 kHz and the companion coda-level metadata from Sharma et al. (2024): click count,  $ICI_1, \dots, ICI_9$ , coda type, clan, social unit, date, and individual identifier where available.

The fixed-suite coda-indexed analyses reconstruct and exclude 18 codas whose published ICI templates extend beyond waveform support, leaving  $n = 1,483$  codas. Phase E retains 44 bouts over this set; second-order TE and the VLMM-inspired dICI comparison use the TE-effective subset of 43 bouts / 1,481 codas after removing one two-coda bout that cannot form  $(t - 2, t - 1, t)$  triples.

*Sharma-anchored click detection..* A detection audit showed that our envelope-peak detector did not recover the published ICI signatures (median absolute ICI error  $\approx 140$  ms; chance-level decoy separation). We therefore use a Sharma-anchored detector: the first click is placed at an energy-maximising anchor  $t_1 = t_0$ , and later clicks are placed at

$$t_k = t_0 + \sum_{i=1}^{k-1} \text{ICI}_i, \quad k > 1. \quad (1)$$

The post-fix median absolute ICI error is  $\approx 0.01$  ms. Because click placement in the main suite is annotation-conditioned, we do not claim de novo click discovery. To show that the click-to-coda findings are not an artifact of this placement, a full de-novo control (§5.2) re-detects click windows from the waveform envelope and re-extracts encoder embeddings there, using neither Sharma intervals nor counts; the click-identity result (T1b) survives it, while the matched-multiset rhythm result (Bridge 6) stays positive but is no longer group-permutation-robust under de-novo timing.

*Embedding extraction..* Per-click windows use a 2 ms pre-onset and 18 ms post-onset span, with 13/18/23 ms sensitivity checks. Clicks are resampled to each encoder’s native rate and mean-pooled; whole-coda embeddings are mean-pooled across the full coda waveform with no internal segmentation. The released configuration records window, sample-rate, detector, prominence, and sensitivity settings.

*Encoder ensemble..* We extract embeddings from eight frozen encoder families with no fine-tuning, taking multiple checkpoints/layers where natural. The Phase A whole-coda inventory analysis uses 23 coda views, giving  $\binom{23}{2} = 253$  encoder-pair comparisons. The click-level suite uses 20 curated click views. Phase F click stretch uses 18 views because two 32 kHz mean-pooled views are unavailable in the aligned per-click stretch arm. All claims are reported as cross-encoder consensus together with agreement statistics; single-view results are companion-only. The view inventory and curation rules are reported in Appendix 2.

*Held-out, blocked cross-validation..* All structural tests are evaluated under cross-validation blocked by Date, social unit, and individual identifier, so that tokens or codas from the same recording session never appear in both train and test. The original click-timescale tests T1–T4 fitted KMeans-on-self and were removed for circularity; their replacements T1b/T2b/T3b/T8 are held-out and have biological targets.

*Consensus tokenisation..* Click- and coda-level tokens are produced by the same two-stage procedure used in Phase A. First, per-encoder KMeans is run on per-click or per-coda embeddings, producing a partition for each eligible encoder view. Phase A uses 23 whole-coda views; the click-level consensus alphabet uses the 20-view click suite. Second, the partitions are combined into a single token assignment by a co-association consensus in the spirit of Strehl and Ghosh (2002). The cluster count  $K$  is selected on the consensus

space by joint silhouette and Calinski–Harabasz scoring, tracked alongside each result, and bootstrap stability is required to be at least 0.5. All click-level statistics (T1b, T2b, T3b, T8, and Bridges 1–6) are computed against the 20-view click consensus token alphabet, and per-encoder versions of each statistic are reported alongside the consensus result so that cross-encoder agreement is visible. The consensus alphabet reduces dependence on any one encoder’s inductive bias; it does not eliminate the possibility of shared biases across frozen audio encoders. Whether the recovered structure is acoustic, and which acoustic property carries it, is a separate question decided by the Phase G gate and by the rhythm-only counterfactuals below.

*Tempo-scaling protocol.* Phase F has two arms. In whole-coda waveform stretch, audio is resampled at  $\{0.8, 1.0, 1.3, 2, 4\} \times$  and re-encoded; in ICI-only stretch, ICIs are scaled while click waveforms are held fixed and re-tiled. We report a matched-tempo cross-tier asymmetry, not a claim that click and coda headline values come from the identical acoustic arm.

*Handcrafted ICI-only baseline.* As a complement to the encoder ensemble, we rerun T1b, Phase A, and Phase E on rhythm-only features. Per-coda vectors contain raw/normalised  $ICI_1, \dots, ICI_9$ , ICI summaries, click count, and duration; per-click vectors add position fraction, neighbouring ICIs, and boundary indicators. Tokenisation,  $K$ -selection, blocked CV, and statistic-specific nulls match the encoder versions where the target is shared. For the rhythm-only Phase A sanity check against published Sharma CodaType, the target and null differ from encoder Phase A and are therefore interpreted separately (§5.7).

*Transfer-entropy estimator sensitivity.* The headline Phase E result uses NSB (Nemenman, Shafee, and Bialek 2002). Section 5.9 reports five additional estimators: Miller–Madow, Jeffreys, plug-in, KSG on a 1-d PCA projection (Kraskov, Stögbauer, and Grassberger 2004), and ordinal-pattern symbolic TE (Staniek and Lehnertz 2008). Four of six are positive; the two negatives are treated as sparse-regime diagnostics rather than hidden headline numbers.

*Acoustic-null recoverability gate (Phase G).* For click-side and mixed click-to-coda statistics, we ask whether the result reproduces from a destructive null that preserves a candidate acoustic carrier and destroys the rest. The click-level nulls are spectrum-matched noise (spectrum-preserving), click-order shuffle (preserves identity, destroys order), envelope-noise fill (preserves the rhythmic envelope only), and cross-coda click replacement (swaps a coda’s clicks for clicks from other codas while preserving the timing skeleton). Coda-level companion nulls include phase-shuffled and time-reversed variants where applicable. Each null is only applied where it is semantically applicable to the statistic (e.g., an order-shuffle null is meaningless against an order-invariant statistic). The gate reports a ratio of real to strongest applicable destructive null and a survival decision; the margin is scale-relative. In the current 1,483-coda run, 5/10 primary Phase G statistics survive the fixed gate and 5/10 are flagged; the flags are interpreted by statistic rather than as a global rejection of lower-tier structure.

*Scale-relative survival rule.* Let  $S_{\text{real}}$  and  $S_{\text{null}}$  be the real value and the strongest applicable destructive-null value. We use the effective margin

$$\Delta_{\text{eff}} = \max\{\Delta_{\text{floor}}, \alpha \max(|S_{\text{real}}|, |S_{\text{null}}|)\}, \quad (2)$$

Claim	Main null/control	Readout
Coda inventory	Phase A pairwise cross-encoder AMI vs. stratified Date $\times$ Unit $\times$ IDN null	$K = 32$ ; median AMI 0.562, null 0.318, lift 0.244; 253/253 BH-FDR pass; bootstrap stability 0.883
Click identity	T1b label shuffle plus Phase G acoustic nulls	NMI 0.410 vs. null 0.032; lift 0.376; 20/20 views positive; median per-encoder lift 0.209
Click order	T2b/Bridge 1 within-coda shuffle plus Phase G	Consensus bigram-null lift 0.0008 bits/token; positional MI lift 0.0076 bits ( $p = 0.005$ ); per-encoder bigram lift positive in 18/20 views but no stable cross-encoder order consensus
Rhythm in codas	Bridge 6 matched click multiset plus group-aware ICI permutation/bootstrap	9,450 pairs from 211 click-multiset groups; $\rho = 0.183$ ; group-aware permutation $p = 0.002$ ; group-bootstrap 95% CI [0.056, 0.372]; $\Delta = 0.144$ ; 23/23 encoders positive
Bout-level sequence	Phase E within-bout shuffle / NSB TE null	Fixed-suite NSB second-order TE lift 0.132 bits; bigram entropy lift 3.304 bits; 139/139 representation/tokenisation variants pass NSB-TE; biological unit = same 43-bout set
Rhythm-only upper tier	Handcrafted ICI and VLMM-inspired dICI baselines under the same TE-effective Phase E protocol	Handcrafted rhythm Phase E lift $-0.419$ ; VLMM-inspired dICI lift $-0.196$ ; encoder consensus is positive under the same 43-bout / 1,481-coda TE-effective sample

**Table 1**

Main-text control map. Phase A reports pairwise cross-encoder AMI among emergent whole-coda VQ partitions against a stratified Date  $\times$  Unit  $\times$  IDN null; NMI to Sharma coda type is only a descriptive sanity check. The 139 Phase E variants are non-independent representation/tokenisation robustness variants; the biological unit is the same 43-bout set. Bridge 6 now reports group-aware robustness rather than relying only on a pair-level shuffle.

with  $\Delta_{\text{floor}} = 0.002$  and  $\alpha = 0.15$ . A statistic survives Phase G only if  $S_{\text{real}} > S_{\text{null}} + \Delta_{\text{eff}}$  and  $|S_{\text{real}}|/|S_{\text{null}}| > 1.10$ ; for smaller-is-better statistics, the directional inequality is reversed. This compact rule prevents small noise-level effects and near-parity destructive-null reproductions from being counted as survivors.

*Reproducibility..* Code, configurations, seeds, token spaces, estimators, nulls, and gate thresholds are listed for anonymous review in Appendix 2.

#### 4. The Structural Test Suite

The suite was fixed before the final reported runs, after removing earlier circular tests. It separates four claims that are easy to conflate: coda inventory, click identity, click order versus rhythm, and bout-level sequence. Table 1 gives the compact control map; Appendix 1 gives the full null-applicability summary.

*Suite overview..* Phase A tests the coda inventory, Phase C exact click-token reuse, Phase E coda-to-bout sequential dependence, Phase F tempo-scaling, and Phase G acoustic-null recoverability. Bridges 1–6 and T1b/T2b/T3b/T8 locate identity, rhythm, order, and

acoustic recoverability; the ICI-only and VLMM-inspired dICI baselines ask whether rhythm alone carries both tiers.

## 5. Results

We follow the layered question from the introduction. Given the coda inventory summarised in Table 1, we first ask how click-level information supports it. We then isolate the click→coda rule, move to codas as upper-level units, test coda→bout sequence structure, and close with the abstraction gradient. Every number below is consensus across encoders unless stated; per-encoder agreement is reported where the consensus and the encoder-by-encoder picture differ.

### 5.1 Lower tier: clicks carry coda information but are tempo-bound

*Click identity predicts coda identity (T1b).* A coda’s click identities, transferred cross-block, predict its coda label well above a label-shuffle null: NMI 0.410 vs. 0.032, with lift 0.376 computed from the current 1,483-coda fixed run. The click alphabet here is the 20-view consensus tokenisation of §3 (per-encoder KMeans → co-association); whether that alphabet is inheriting structure from gross spectrum, click order, or rhythmic envelope rather than from per-click identity is exactly what the Phase G `spectrum_matched_noise`, `click_order_shuffle`, and `envelope_noise_fill` nulls are designed to test; and T1b survives those controls. The signal is unanimous across the 20 click views, with median per-encoder lift 0.209; each encoder clears its own non-circular null independently. T1b is also identity-specific: it is insensitive to click-order shuffle and drops under cross-coda click replacement, where clicks are swapped between codas while timing is held fixed. Under the fixed Phase G rule, T1b is one of the 5/10 primary survivors and remains the most robust click-identity diagnostic under threshold-sensitivity checks.

*The click-token geometry is low-dimensional, and transfer survives the gate (Bridge 3).* A held-out token-subset transfer test finds low-dimensional click-token geometry: participation ratio  $0.24 \cdot (K - 1)$ , equivalent to roughly two effective dimensions in the click inventory. Bridge 3 has two arms, and the acoustic-null gate separates them. The transfer-lift arm passes the fixed Phase G rule, while the participation-ratio arm is treated as a descriptive accompaniment rather than a load-bearing statistic when it is recoverable from spectrum-preserving nulls. The result is consistent with compact click-token structure at the click tier, with the fixed-gate support carried by the transfer-lift arm and interpreted alongside T1b rather than alone.

*Click identity is rate-dependent (Phase F).* Under matched tempo-scaling (0.8×, 1.3×, 2×, 4×), encoder-derived whole-waveform click inventories cluster poorly against the unstretched reference: ARI  $\approx 0.07$  across all 18 eligible encoder views.

### 5.2 The click-to-coda rule: unordered set plus rhythm

*Click order is consensus-absent (T2b).* Beyond a within-coda click shuffle, the consensus bigram-null lift is 0.0008 bits/token and the positional-MI lift is 0.0076 bits ( $p = 0.005$ ). The positional-MI probe is detectable but tiny; together these values do not support a stable ordered click rule once the click multiset is known.

*Per-encoder picture: weak, encoder-dependent (Bridge 1)..* The honest cross-encoder report is more nuanced than the consensus alone. Eighteen of 20 encoders show a nominally positive bigram–null lift on their own tokens, but the encoders disagree on what that order is: Bridge 1’s per-encoder click-tier contiguous Markov depth splits 11/20 at depth 0, with the largest single estimate reaching depth 2. Combined with the near-zero consensus result, this means some encoders pick up weak order signal, but the signals disagree across encoders and wash out in aggregation. A stable cross-encoder click-order rule is not present.

*Coda-label and context probes do not rescue an order claim (T3b, T8)..* The held-out coda-label probe is above its shuffled-label null, but ordered click embeddings do not beat a bag baseline. Under the fixed Phase G rule, T3b is treated as a diagnostic of coda-label information in the click inventory rather than as evidence for stable ordered productivity. The T8 context-position probe is small and should be read as a weak context diagnostic, not as an order rule. These diagnostics support coda-label information in the click inventory, not a stable ordered-productivity claim.

*Every click contributes roughly equally (Bridge 5)..* Per-click ablation is near-uniform: normalised entropy  $\approx 0.99$ , max/mean ratio 1.27, and mean per-click shift 0.031. There is no dominant “head” click.

*Rhythm directly contributes to coda identity (Bridge 6)..* The strongest positive evidence for the bag-plus-rhythm picture is direct rather than inferential. Bridge 6 matches coda pairs on their exact click-token multiset, holding click inventory fixed, and tests whether ICI-pattern distance tracks coda-embedding distance. The current fixed-suite result uses 9,450 matched pairs from 211 exact click-token-multiset groups. The association is positive across all 23 encoder views:  $\rho = 0.183$  with group-aware permutation  $p = 0.002$ , group-bootstrap median  $\rho = 0.181$  and 95% CI [0.056, 0.372], and high-versus-low ICI-distance contrast  $\Delta = 0.144$ . Per-encoder agreement is also uniform: 23/23 encoders are positive, with median per-encoder  $\rho = 0.159$ . Because the robustness check now permutes/bootstrap-samples at the click-multiset group level, the result no longer rests only on a pair-level shuffle. The correct reading is still structural rather than behavioural: with click multiset held identical, rhythm moves the coda representation beyond the inventory of clicks present.

*Rhythm-only handcrafted baseline recovers much of T1b..* Replacing encoder consensus embeddings with the handcrafted ICI-only feature space and rerunning T1b yields NMI lift 0.261, compared with encoder lift 0.376 ( $\Delta = 0.115$ ). Timing alone therefore recovers much click-to-coda predictive structure, but not at parity; its upper-tier failure in §5.4 makes the substrate-change reading a measured comparison.

*Full de-novo click-detection control..* Because the main click suite places windows at Sharma-anchored times, a fair question is whether the click-to-coda signal is an artifact of annotation-conditioned placement. We therefore rerun the two load-bearing click-timing tests, T1b and Bridge 6, after detecting click windows directly from the waveform envelope and re-extracting encoder per-click embeddings at those de-novo windows; this arm uses neither Sharma inter-click intervals nor Sharma click counts. Crucially, envelope detection does not reproduce the published ICI annotations (the detection audit above), so the de-novo windows are genuinely independent of Sharma timing, and a surviving signal rules out annotation-conditioned circularity rather than re-deriving

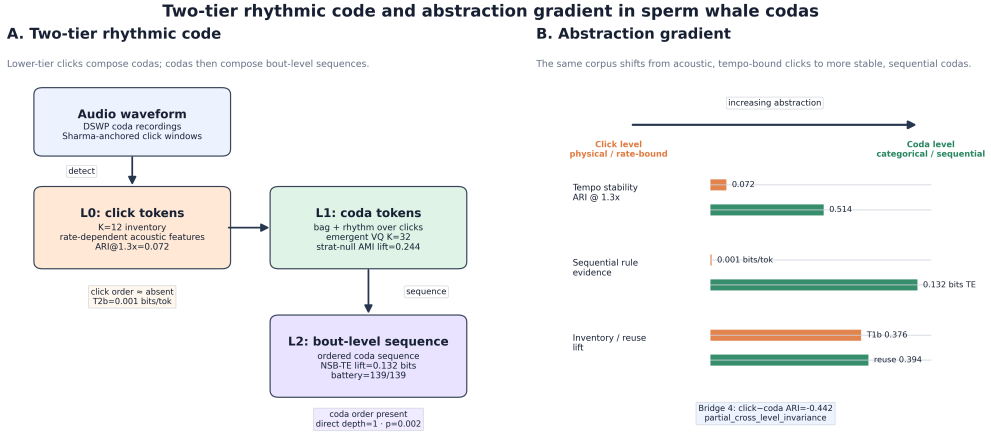


**Figure 1**

Two-tier rhythmic structure and abstraction gradient. Click tokens compose into coda tokens through unordered inventory plus rhythm; coda tokens then participate in bout-level sequential dependence. At 1.3x, click ARI is 0.074, same-arm coda ARI is ≈ 0.428, and ICI-only coda ARI is ≈ 0.516.

it. On the same 1,483 codas (the same 18 Sharma-truncated codas excluded), envelope detection yields 9,151 de-novo clicks; the de-novo click consensus uses  $K = 12$  over 18 click views (cross-view mean ARI 0.190), with 21 coda views for the matched-multiset test. For T1b, de-novo click identity still predicts coda label far above the label-shuffle null: median NMI 0.379 vs. null 0.027, lift 0.347, with 18/18 click encoders beating their own nulls (median per-encoder lift 0.285). This is close to the Sharma-anchored encoder result (lift 0.376) and directly refutes click-window circularity for click identity. For Bridge 6, the de-novo matched-multiset test (4,045 pairs from 188 click-token-multiset groups) gives  $\rho = 0.196$  with pair-shuffle  $p = 0.002$ , high-versus-low ICI-distance contrast  $\Delta = 0.160$ , and 21/21 coda encoders positive; the group bootstrap is positive (median  $\rho = 0.203$ , 95% CI [0.108, 0.293]). The stricter within-click-bag group permutation, however, does not pass under de-novo timing ( $p = 0.365$ ). The reading is therefore asymmetric: the de-novo control strongly refutes circularity for click identity (T1b lift 0.347 vs. 0.376), and gives positive, encoder-consistent, bootstrap-positive but not group-permutation-robust support for rhythm beyond the click-token bag (Bridge 6).

*The lower-tier evidence points to inventory plus rhythm..* Together, T2b/Bridge 1 show no stable cross-encoder order; Bridge 5 shows near-uniform click contribution; Bridge 6 shows that ICI structure still moves coda embeddings when click multiset is fixed; the rhythm-only baseline recovers much of T1b while failing at the bout tier; and the click-identity result survives full de-novo click detection (§5.2). The lower tier is therefore best described as which clicks are present plus their inter-click timing.

**5.3 Upper units: codas are recurring, partly rate-stable representation-level categories**

*A representation-level coda inventory emerges (Phase A)..* Phase A measures agreement among emergent whole-coda partitions, not agreement with published Sharma coda-type labels. At  $K = 32$ , median pairwise cross-encoder AMI is 0.562 over 253 encoder pairs; the Date

$\times$  Unit  $\times$  IDN-stratified null median is 0.318, giving lift 0.244. All 253/253 tests pass BH-FDR, and bootstrap stability is 0.883. NMI to Sharma coda type is descriptive only; the stratified null is deliberately conservative because Date/Unit/IDN already carries real structure.

*Coda strings recur (Phase C)..* Exact click-token coda strings recur at fraction 0.394 versus 0.033 for a length-matched multinomial null, giving lift 0.362; the median per-encoder lift is 0.097. The result supports recurrence of click-token strings under the fixed 1,483-coda denominator.

*Coda identity is substantially more rate-stable than click identity (Phase F, Bridge 4)..* Under matched tempo-scaling, whole-waveform click inventories are much less stable than coda inventories. At  $1.3\times$ , click ARI is 0.074, same-arm whole-waveform coda ARI is  $\approx 0.428$ , and ICI-only coda ARI is  $\approx 0.516$ ; at  $2\times$ , the two coda ARIs are  $\approx 0.460$  and  $\approx 0.434$ . Thus both coda arms remain substantially more stable than the whole-waveform click arm. The robust claim is the click-coda asymmetry, not perfect coda invariance.

#### 5.4 Bout-level sequential dependence

*Codas show bout-level sequential dependence (Phase E, Bridge 1)..* We use sequential dependence operationally: statistically reliable dependence among coda tokens, not syntax or semantics. We distinguish retained-bout accounting from second-order-TE accounting. Bridge 1 uses 44 retained bouts / 1,483 codas under `min_codas_per_bout=2`. Second-order TE and the VLMM-inspired dICI comparison use 43 bouts / 1,481 codas, because one retained bout, `09/03/2010__D`, has only two codas and cannot form triples ( $t-2, t-1, t$ ).

Under this fixed TE-effective protocol, NSB second-order transfer entropy has lift 0.132 bits ( $p = 0.002$ ), and bigram entropy lift is 3.304 bits. The 139 eligible coda-token streams are representation/tokenisation robustness variants over the same bout set, not independent biological samples: 139/139 pass NSB-TE, 139/139 pass the bigram test, 138/139 pass the trigram test after BH correction, and the Date  $\times$  Unit  $\times$  IDN sensitivity battery passes 139/139. Bridge 1's direct coda-within-bout contiguous Markov estimate is depth 1 on the 44 retained bouts; the candidate battery supports second-order evidence under the fixed NSB suite, but the direct contiguous depth-2 estimate is power-limited. The load-bearing claim is therefore sequential dependence at the coda tier, with depth-2 support tied specifically to the fixed NSB TE battery and the direct depth-1 estimate treated as a conservative floor.

Sparse-context accounting is explicit: with  $K = 32$ , the TE-effective sample has 1,395 triples and 166/1024 occupied two-step contexts (median count 2; 30 contexts have count at least 10; full counts in §5.9). These counts are why we report second-order evidence under the fixed NSB suite rather than an estimator-invariant direct Markov-depth result. The estimator panel is diagnostic: four of six variants are positive, while Jeffreys and ordinal-pattern TE are negative in this sparse regime.

*A stronger rhythm-only counterfactual still fails Phase E..* To test whether the simple rhythm-only failure reflects weak representation rather than substrate change, we run a dICI n-gram / variable-length-Markov-inspired rhythm-only baseline, motivated by prior dICI patterning work such as Hersh et al. (2022). Each within-coda dICI sequence is quantile-binned into a 4-symbol alphabet; unigram, bigram, and trigram bags produce 84 features; KMeans clusters at  $K = 32$ ; and the TE-effective filter, ordering, NSB estimator,

and within-bout shuffle null match encoder Phase E. The Phase E-relevant quantity is lift over the within-bout shuffle null, not raw TE. The simple handcrafted rhythm baseline gives lift  $-0.419$ , the richer VLMM-inspired dICI baseline gives lift  $-0.196$ , while encoder consensus gives  $+0.132$  ( $p = 0.002$ ) on the same 43-bout / 1,481-coda TE-effective sample. The two rhythm-only counterfactuals tested here may carry first-order transitions, but they do not recover the second-order lift that defines Phase E.

### 5.5 The abstraction gradient

Under matched tempo-scaling factors, encoder-derived whole-waveform click identity is strongly disrupted while coda identity remains substantially more stable. A tempo-bound lower unit therefore becomes a more representation-level upper unit across one combinatorial step: a measured phonetics-to-phonology-like abstraction gradient. The claim is cross-tier asymmetry, not perfect coda invariance.

### 5.6 Cross-encoder convergence

The main pillars are not single-view artifacts: Phase A passes across 253/253 coda-view pairs, T1b is positive in 20/20 click views, Phase C beats its null with median per-encoder lift 0.097, and Bridge 6 is positive in 23/23 coda views. The exception is click order, where the consensus lift is near zero and Bridge 1 splits 11/20 at click-tier depth 0 with maximum depth 2.

### 5.7 Rhythm-only Phase A sanity check

The rhythm-only Phase A number is not the same target as encoder Phase A. Encoder Phase A measures pairwise cross-encoder AMI among emergent whole-coda VQ partitions against a Date  $\times$  Unit  $\times$  IDN-stratified null. The rhythm-only sanity check instead runs KMeans with  $K = 32$  on handcrafted Sharma-anchored rhythm features and measures AMI against the published Sharma CodaType label.

In the current run, AMI against encoder consensus is 0.223208, AMI against Sharma CodaType is 0.807923, the Date  $\times$  Unit-stratified null against Sharma is 0.158326, and the lift against that Sharma-label null is 0.649598. This number is high because Sharma CodaType is itself ICI/rhythm-defined. It does not mean rhythm-only representations recover the upper-tier sequential dependence. The decisive substrate-change contrast is Phase E: handcrafted rhythm Phase E lift  $-0.419$ , VLMM-inspired dICI lift  $-0.196$ , and encoder Phase E lift  $+0.132$  on the same TE-effective sample.

### 5.8 VLMM-inspired dICI rhythm-only Phase E counterfactual

A natural worry about the substrate-change reading is that the rhythm-only Phase E failure could reflect representational inadequacy rather than a genuine substrate change. We test this directly with a richer rhythm representation modelled as a dICI n-gram / variable-length-Markov-inspired baseline, motivated by prior dICI patterning work such as Hersh et al. (2022). The code does not implement or import a named prior VLMM method verbatim; the baseline is a reviewer-facing rhythm-only counterfactual.

Each within-coda dICI sequence is binned into corpus-wide quantile symbols over a 4-symbol alphabet, then aggregated as a bag of unigrams, bigrams, and trigrams for 84 features per coda. KMeans clusters at the same consensus  $K$  used by encoder Phase A ( $K = 32$ ). The TE-effective bout filter, coda ordering, minimum-codas-per-bout cut,

NSB transfer-entropy estimator, and within-bout shuffle null are all bit-identical to those used by encoder Phase E, so the resulting TE lift is directly comparable line for line. The retained-bout filter admits 44 bouts / 1,483 codas, but second-order TE/VLMM uses 43 bouts / 1,481 codas because the retained bout 09/03/2010\_\_D has only two codas and cannot form triples.

The Phase E-relevant quantity is the TE lift over the within-bout shuffle null, not the raw TE. The richer rhythm representation produces negative lift  $-0.196$  bits with  $p = 1.000$  against 200 shuffles. The simple handcrafted-rhythm baseline gives an even more negative lift of  $-0.419$  bits at the same  $p$ . The encoder consensus Phase E lift is  $+0.132$  bits with  $p = 0.002$  on the same 43-bout / 1,481-coda TE-effective sample.

The two rhythm-only baselines and the encoder consensus sit on opposite sides of zero, not at smaller and larger magnitudes on the same side. The right reading of this panel is that rhythm-only representations can support first-order coda-to-coda transitions but they do not carry second-order sequential dependence in which the  $t - 2$  token adds information beyond what  $t - 1$  already provides. The encoder ensemble does carry that second-order signal under the fixed NSB suite, and adding rhythm-representation richness moves the rhythm-only deficit toward zero but does not change its sign. Rhythm-representation richness is therefore not what gates the bout-level finding, and the substrate-change reading is supported empirically against its strongest counterfactual.

### 5.9 Phase E transfer-entropy estimator sensitivity

The reportable Phase E headline is the value produced by the fixed structural suite: NSB second-order transfer-entropy lift of  $0.132$  bits ( $p = 0.002$ ). We use NSB (Nemenman, Shafee, and Bialek 2002) because the depth-2 categorical setting is sparse: a  $K = 32$  coda alphabet gives 1,024 possible bigram contexts, of which 166 are occupied on the 43-bout / 1,481-coda TE-effective sample. The sample contains 1,439 transitions and 1,395 second-order triples; all 32 one-step contexts are occupied; there are 172 unique bigrams and 326 unique trigrams; two-step context counts have min 1, median 2, max 105, with 86 contexts at count at least 2, 41 at least 5, and 30 at least 10. To check that the sign is not solely an NSB artefact, we also ran a six-estimator sensitivity panel on the same coda-token streams. That panel uses a common recalibrated preprocessing path across estimators, so its NSB row is  $0.148$  rather than the headline  $0.132$ ; this is a protocol variant, not a competing headline number, and the sign and interpretation are unchanged.

The full panel is NSB ( $0.148$ ), Miller–Madow ( $0.339$ ), naive plug-in ( $0.350$ ), KSG with  $k = 4$  (Kraskov, Stögbauer, and Grassberger 2004) on a 1-d PCA projection of consensus coda embeddings ( $+0.014$ ), Jeffreys (Dirichlet- $1/2$  prior;  $-0.186$ ), and ordinal-pattern symbolic TE (Staniek and Lehnertz 2008) with  $m = 3$ ,  $\tau = 1$  on the same projection ( $-0.020$ ). Four of six estimators give positive lifts; the two negatives are informative failure modes in this sparse categorical regime, not contradictions of the fixed-suite result. The VLMM-inspired dICI rhythm-only baseline is a separate substrate counterfactual, not an estimator-sensitivity row.

*Jeffreys..* The Dirichlet- $1/2$  prior places half a pseudocount on every cell of the conditional distribution. With a 32-token alphabet at depth 2, every empty bigram context receives a non-trivial smoothing mass; in our regime the cumulative smoothing mass swamps the actual conditional dependency in the data, and the estimated TE is pushed below

the within-bout shuffle null. The same prior is benign at depth 1; the negative reading is regime-specific, not a refutation of the headline.

*Ordinal-pattern TE.* The symbolic TE estimator on a 1-d PCA projection of coda embeddings discards exactly the categorical structure that the bout-level result relies on: it sees only the rank order of three projected values, not the categorical label of the coda. Section 5.4 shows independently that rhythm-only substrates give negative TE lifts; so any estimator that throws away categorical identity, as ordinal-pattern TE on a low-dimensional projection effectively does, is expected to give a non-positive lift. The ordinal-pattern result is consistent with, not contradictory to, the substrate-change finding.

## 6. Discussion

The evidence supports a narrow claim: sperm-whale codas exhibit a two-tier combinatorial organisation in which the composition rule changes between adjacent levels. At the lower tier, clicks form codas through inventory plus rhythm: click order is unstable, click contributions are near-uniform, group-robust Bridge 6 keeps matched-multiset codas separated by ICI pattern, and an ICI-only baseline recovers much of T1b without reaching encoder parity. At the upper tier, codas recur and sequence within bouts: the two rhythm-only counterfactuals tested here fail Phase E by sign, while coda-token streams retain positive second-order sequential-dependence lift under the fixed NSB suite. The acoustic-null gate should be read statistic by statistic: in the current 1,483-coda run, 5/10 primary Phase G statistics survive the fixed rule and 5/10 are flagged. The load-bearing lower-tier claims rely on the surviving identity/rhythm diagnostics; flagged diagnostics are interpreted only as non-support for stronger symbolic or order claims.

*What we claim.* A representation-level two-tier combinatorial structure in coda communication; a click inventory whose identity carries coda-relevant information beyond destructive acoustic nulls; an unordered-inventory-plus-rhythm composition rule at the click→coda tier, with rhythm established directly by Bridge 6's matched-multiset structural association and group-aware robustness as well as by elimination; a representation-level whole-coda inventory supported by pairwise cross-encoder AMI above a Date × Unit × IDN-stratified null; more rate-stable representation-level codas under matched tempo-scaling factors; operational sequential dependence at the bout level; a measurable abstraction gradient across the click→coda step; and cross-encoder convergence on the primary pillars.

*What we do not claim.* We do not claim “featural phonology” in the strong sense: low rank is consistent with a low-dimensional code but does not establish discrete contrastive features. We do not claim a click-order rule, language, semantics, or behavioural/perceptual demonstration of any structural finding. As argued in the introduction, these abstentions are scope decisions appropriate to design-feature analysis, not concessions that the structural findings fall outside the study of language.

*Implications, in descending order of support.* (i) *Duality-of-patterning-like structure.* A finite lower inventory whose units are not themselves the communicatively salient unit combines into a larger inventory of units that are representation-level, recurring, and sequentially structured. This is consistent with the formal signature of duality of patterning (Hockett 1960); because we do not show coda semantics, the honest

formulation is representation-level evidence consistent with duality-of-patterning-like organization. (ii) *A combinatorial design different from canonical segmental language models.* Human language relies heavily on ordered combination at several levels, but not every linguistic contrast is reducible to order alone. Here the composition rule changes between tiers: the lower tier is unordered inventory plus rhythm, and the upper tier is sequentially structured. This is not whales reinventing human phonology; it is a structurally distinct solution to the combinatorial-coding problem, and one that the order-centric assumptions built into many sequence models would miss by construction. (iii) *Rhythm as a major contrastive substrate, directly tested.* The lower-tier contrasts are carried substantially by inter-click timing rather than by an ordered string of spectral segments. This is established by Bridge 6’s matched-multiset test and group-aware robustness, and by the rhythm-only handcrafted baseline recovering much of T1b, though not at encoder parity. (iv) *An empirical handle on the phonetics-to-phonology boundary.* Encoder-derived whole-waveform click identity is rate-dependent; coda identity is substantially more rate-stable under matched tempo-scaling. The emergence of representation-level abstraction can be measured across a single combinatorial step. (v) *A prerequisite for productivity, not a demonstration of it.* Hierarchical discreteness is the architecture that could support open-ended, productive communication. We have not shown productivity itself. (vi) *The substrate of composition changes between tiers.* The rhythm-only baseline recovers substantial Tier-1 structure (T1b lift +0.261 versus encoder +0.376; §5.7 explains the separate rhythm-only Phase A sanity check), but its Tier-2 lift collapses (−0.419 for Phase E), and the richer VLMM-inspired dICI baseline remains negative (−0.196). The substrate-change comparison is therefore a sign contrast at the upper tier: +0.132 bits under the encoder ensemble versus −0.196 for the strongest rhythm-only counterfactual and −0.419 for the simple rhythm-only baseline on the same 43-bout / 1,481-coda TE-effective sample.

*Methodological transfer.* The apparatus behind these claims is not specific to whales. Inducing a token alphabet from a frozen encoder, requiring agreement across independently trained encoders, attaching a non-circular null to every structural statistic, and then asking whether a destructive acoustic null can counterfeit the result, is a general recipe for distinguishing combinatorial structure from acoustic similarity in any setting where symbols must be discovered rather than read off. The same gate that flags 5/10 of our click-level statistics is what licenses the surviving ones; we would expect this discipline to be useful wherever compositionality and topographic-similarity metrics are applied to induced rather than given alphabets, including low-resource speech and other animal-communication corpora.

## 7. Conclusion

Sperm whale codas reveal a narrow, representation-level two-tier architecture. Click identity carries coda-relevant information, but stable ordered click rule is not supported: consensus order statistics are near zero, per-encoder order signals disagree, and ordered click embeddings do not beat a bag baseline. The positive lower-tier result is inventory plus rhythm. At the upper tier, codas recur and sequence within bouts: encoder coda-token streams retain positive second-order sequential-dependence lift under the fixed NSB suite, while handcrafted rhythm and VLMM-inspired dICI alternatives remain negative under the same protocol. Matched tempo-scaling ties the tiers together by showing rate-bound encoder-derived click identity but more stable coda identity. The claim is representation-level evidence consistent with a duality-of-patterning-like organization, not language, semantics, perception, or human-like phonemes. Methodologically,

the paper offers computational linguistics a portable discipline for the same problem in any induced-token setting: distinguishing genuine combinatorial structure from acoustic similarity through cross-encoder consensus, per-statistic nulls, and acoustic-null recoverability gates. Establishing that a non-human system carries one of language's defining design features, and identifying exactly which combinatorial substrate carries it, is, we argue, squarely a question for the computational study of language.

## Limitations

*Representational, not behavioural..* All claims describe the geometry of frozen-encoder embeddings under explicit nulls and gates. They are not perceptual or behavioural measurements; whether whales use these contrasts remains an open behavioural question.

*Single population..* The data are from one population, Dominica. Cross-population replication is necessary before making species-level claims about sperm whale coda structure.

*Bout sample is power-limited..* The bout-tier claim uses a small sample. Bridge 1 retains 44 bouts / 1,483 codas, while second-order TE/VLMM uses 43 bouts / 1,481 codas because one retained two-coda bout cannot form  $(t - 2, t - 1, t)$  triples. The candidate TE battery supports second-order evidence under the fixed NSB suite, but the direct contiguous-depth estimator returns depth 1; we therefore do not claim depth 2 from any single bout-set estimate. A second population, or longer recordings, would be needed to pin a direct contiguous estimate at depth 2 or above.

*Shared encoder bias is mitigated, not eliminated..* The encoder ensemble spans bioacoustic, general-audio, music/audio, and speech pretraining regimes, but frozen audio encoders may still share rhythm-sensitive biases. Cross-encoder agreement and acoustic nulls reduce this risk but do not remove it. A click-specialised front end remains a necessary next step.

*16 kHz sample-rate cap..* The source audio used here is 16 kHz. Perch and VampNet provide 32 kHz input-rate sanity checks on resampled 16 kHz audio, but they do not restore high-frequency information absent from the source waveform. Higher-rate audio encoders or click-specialised front ends are needed to measure how much segmental click identity is hidden at the click tier.

*Partial, not perfect, rate-stability..* The robust claim is the click-coda asymmetry under matched tempo-scaling, not full Tier 2 invariance.

*Bridge 6 group dependence..* Bridge 6 reports 9,450 matched coda pairs from 211 exact click-token-multiset groups. Pairs are not independent biological samples, so the revised analysis uses group-aware permutation and group bootstrap rather than leaning on the parametric Spearman or pair-level shuffle alone. The group-aware permutation remains significant ( $p = 0.002$ ), and the group-bootstrap 95% CI is [0.056, 0.372]. Under fully de-novo click timing (§5.2), the same matched-multiset association stays positive and encoder-consistent ( $\rho = 0.196$ , 21/21 coda views, group-bootstrap CI [0.108, 0.293]) but no longer clears the within-group permutation ( $p = 0.365$ ); we therefore treat rhythm-

beyond-bag as group-robust under Sharma-anchored timing and positive-but-not-group-permutation-robust under de-novo timing.

*Dependence on prior ICI annotation..* Click positions are computed from cumulative published ICIs (Sharma et al. 2024) from an energy-maximising anchor. We verify alignment to the published intervals but do not independently validate the biological correctness of the underlying annotation.

*Status of click-level statistics..* The fixed acoustic-null gate leaves 5/10 primary statistics surviving and 5/10 flagged. These outcomes should not be read as confirmation of click-level symbolicity in the strong linguistic sense. A low-rank inventory with identity-bearing units is not the same as discrete contrastive features in the strong linguistic sense, and we do not claim the latter.

### Ethical Considerations

This work is a secondary analysis of pre-existing audio and metadata collected by the Dominica Sperm Whale Project under permits to the original investigators; no new animal data were collected for this study. The audio recordings concern a vulnerable species, and we encourage caution against over-interpreting structural findings as evidence of language or semantic content; such overclaims, in our view, do harm both to the science and to the species, by raising and then disappointing public expectations. We release no individually-identifying metadata that is not already public in the source dataset. The statistical test suite, null choices, and reporting rules were fixed before the final reported runs; no result reported here was selected from a wider set after inspecting the final outcomes.

### References

- Andreas, Jacob. 2019. Measuring compositionality in representation learning. In *International Conference on Learning Representations*.
- Baevski, Alexei, Yuhao Zhou, Abdelrahman Mohamed, and Michael Auli. 2020. wav2vec 2.0: A framework for self-supervised learning of speech representations. In *Advances in Neural Information Processing Systems*, volume 33, pages 12449–12460.
- Benjamini, Yoav and Yoel Hochberg. 1995. Controlling the false discovery rate: A practical and powerful approach to multiple testing. *Journal of the Royal Statistical Society: Series B (Methodological)*, 57(1):289–300.
- Berwick, Robert C., Kazuo Okanoya, Gabriel J. L. Beckers, and Johan J. Bolhuis. 2011. Songs to syntax: The linguistics of birdsong. *Trends in Cognitive Sciences*, 15(3):113–121.
- Brighton, Henry and Simon Kirby. 2006. Understanding linguistic evolution by visualizing the emergence of topographic mappings. *Artificial Life*, 12(2):229–242.
- Chaabouni, Rahma, Eugene Kharitonov, Diane Bouchacourt, Emmanuel Dupoux, and Marco Baroni. 2020. Compositionality and generalization in emergent languages. In *Proceedings of the 58th Annual Meeting of the Association for Computational Linguistics*, pages 4427–4442, Association for Computational Linguistics.
- Chen, Sanyuan, Yu Wu, Chengyi Wang, Shujie Liu, Daniel Tompkins, Zhuo Chen, Wanxiang Che, Xiangzhan Yu, and Furu Wei. 2023. BEATs: Audio pre-training with acoustic tokenizers. In *Proceedings of the 40th International Conference on Machine Learning*, volume 202 of *Proceedings of Machine Learning Research*, pages 5178–5193.
- Clarke, Esther, Ulrich H. Reichard, and Klaus Zuberbühler. 2006. The syntax and meaning of wild gibbon songs. *PLoS ONE*, 1(1):e73.
- Garcia, Hugo Flores, Prem Seetharaman, Rithesh Kumar, and Bryan Pardo. 2023. VampNet: Music generation via masked acoustic token modeling. In *Proceedings of the 24th International Society for Music Information Retrieval Conference*, pages 699–707.

- Gero, Shane, Hal Whitehead, and Luke Rendell. 2016. Individual, unit and vocal clan level identity cues in sperm whale codas. *Royal Society Open Science*, 3(1):150372.
- Ghani, Bashar, Tom Denton, Stefan Kahl, and Holger Klinck. 2023. Global birdsongs embeddings enable superior transfer learning for bioacoustic classification. *Scientific Reports*, 13:22876.
- Goffinet, Jack, Samuel Brudner, Richard Mooney, and John Pearson. 2021. Low-dimensional learned feature spaces quantify individual and group differences in vocal repertoires. *eLife*, 10:e67855.
- Hagiwara, Masato. 2023. AVES: Animal vocalization encoder based on self-supervision. In *Proceedings of the IEEE International Conference on Acoustics, Speech and Signal Processing*, pages 6157–6161.
- Hersh, Talia A., Shane Gero, Luke Rendell, and Hal Whitehead. 2022. Evidence from sperm whale clans of symbolic marking in non-human cultures. *Proceedings of the National Academy of Sciences*, 119(37):e2201692119.
- Hockett, Charles F. 1960. The origin of speech. *Scientific American*, 203(3):88–96.
- Hsu, Wei-Ning, Benjamin Bolte, Yao-Hung Hubert Tsai, Kushal Lakhota, Ruslan Salakhutdinov, and Abdelrahman Mohamed. 2021. HuBERT: Self-supervised speech representation learning by masked prediction of hidden units. *IEEE/ACM Transactions on Audio, Speech, and Language Processing*, 29:3451–3460.
- Kraskov, Alexander, Harald Stögbauer, and Peter Grassberger. 2004. Estimating mutual information. *Physical Review E*, 69(6):066138.
- Lazaridou, Angeliki, Karl Moritz Hermann, Karl Tuyls, and Stephen Clark. 2018. Emergence of linguistic communication from referential games with symbolic and pixel input. In *International Conference on Learning Representations*.
- Nemenman, Ilya, Fariel Shafee, and William Bialek. 2002. Entropy and inference, revisited. In *Advances in Neural Information Processing Systems*, volume 14.
- Prat, Yossi, Leonie Azoulay, Roi Dor, and Yossi Yovel. 2017. Crowd vocal learning induces vocal dialects in bats: Playback of conspecifics shapes fundamental frequency usage by pups. *PLoS Biology*, 15(10):e2002556.
- Radford, Alec, Jong Wook Kim, Tao Xu, Greg Brockman, Christine McLeavey, and Ilya Sutskever. 2023. Robust speech recognition via large-scale weak supervision. In *Proceedings of the 40th International Conference on Machine Learning*, volume 202 of *Proceedings of Machine Learning Research*, pages 28492–28518.
- Rendell, Luke and Hal Whitehead. 2003. Vocal clans in sperm whales. *Proceedings of the Royal Society of London. Series B: Biological Sciences*, 270(1512):225–231.
- Resnick, Cinjon, Abhinav Gupta, Jakob Foerster, Andrew M. Dai, and Kyunghyun Cho. 2020. Capacity, bandwidth, and compositionality in emergent language learning. In *Proceedings of the 19th International Conference on Autonomous Agents and MultiAgent Systems*, pages 1125–1133.
- Sainburg, Tim, Benjamin Theilman, Marvin Thielk, and Timothy Q. Gentner. 2020. Parallels in the sequential organization of birdsong and human speech. *Nature Communications*, 11:3636.
- Sainburg, Tim, Marvin Thielk, and Timothy Q. Gentner. 2020. Finding, visualizing, and quantifying latent structure across diverse animal vocal repertoires. *PLoS Computational Biology*, 16(10):e1008228.
- Schreiber, Thomas. 2000. Measuring information transfer. *Physical Review Letters*, 85(2):461–464.
- Sharma, Pratyusha, Shane Gero, Roger Payne, David F. Gruber, Daniela Rus, Antonio Torralba, and Jacob Andreas. 2024. Contextual and combinatorial structure in sperm whale vocalisations. *Nature Communications*, 15:3617.
- Staniek, Matthias and Klaus Lehnertz. 2008. Symbolic transfer entropy. *Physical Review Letters*, 100(15):158101.
- Strehl, Alexander and Joydeep Ghosh. 2002. Cluster ensembles: A knowledge reuse framework for combining multiple partitions. *Journal of Machine Learning Research*, 3:583–617.
- Watkins, William A. and William E. Schevill. 1977. Sperm whale codas. *Journal of the Acoustical Society of America*, 62(6):1485–1490.

## 1. Null-Applicability Matrix

### Phase 1 null-applicability matrix

Rows are biological tiers. Empty non-applicable cells are omitted here; the Markdown/LaTeX source keeps the full audit table.

Click -> coda	<b>T1b click-&gt;coda identity</b> SURVIVES: Phase G: T1b cross block transfer: survives	<b>T2b click order /position</b> FLAGGED: Phase G: T2b bigram lift: flagged; T2b positional mi: survives	<b>T3b click-&gt;coda label</b> SURVIVES: Phase G: T3b coda label probe: survives	<b>Bridge 2 functional substitution</b> FLAGGED: Phase G: B2 partial spearman: flagged; B2 substitution minus same label: flagged
	<b>Bridge 3 featural structure</b> FLAGGED: Phase G: B3 featural transfer lift: survives; B3 featural pr ratio: flagged	<b>Bridge 5 click ablation</b> FLAGGED: Phase G: B5 max to mean ratio: flagged	<b>Phase C click-token reuse</b> INFO: Phase G: phaseC reuse fraction: info Primary null: multinomial lift=0.362	
Coda -> bout	<b>Phase A emergent coda VQ</b> SURVIVES: stratified Date+Unit+IDN null AMI lift=0.244; FDR=1.000	<b>Phase E coda sequence</b> SURVIVES: bout-block shuffle + NSB+TE battery bigram=1.000, trigram=1.000, TE=1.000	<b>TE estimator sensitivity</b> INFO: estimator sensitivity positive=46	
Rule change between tiers	<b>Bridge 4 stretch rule</b> NOT GATED: ICI-only coda stretch vs click waveform stretch click-AMI=0.072, coda AMI=0.514	<b>Bridge 6 rhythm rule</b> SURVIVES: matched click-bag group null rho=0.183; group-p=0.002	<b>Handcrafted rhythm control</b> INFO: handcrafted rhythm baseline T1b lift=0.259; Phase E TE lift=0.419	

■ survives   
 ■ flagged   
 ■ not gated   
 ■ info

**Figure A.2:** Phase 1 null-applicability matrix. Rows are biological tiers; cells name the active null or control. Cell text marks survive, flagged, not Phase-G gated, or informational outcomes, so the matrix remains interpretable without relying only on colour.

## 2. Per-Test Protocol Summary

*Tokenisation implementation details..* The anonymous release configuration records the exact  $K$  grid, KMeans number of initialisations, maximum iterations, convergence tolerance, random seeds, and encoder checkpoint identifiers used for each view. For each encoder view, KMeans produces a partition over the relevant click or coda embeddings; the co-association matrix entry  $A_{ij}$  is the fraction of encoder partitions assigning items  $i$  and  $j$  to the same cluster; and the final consensus partition is selected on this co-association space using the same silhouette/Calinski-Harabasz rule as Phase A. For predictive or held-out tests, tokenisation choices are made without using held-out biological labels, and all reported nulls preserve the same blocked fold structure.

*Reproducibility configuration..* The fixed-suite runner reconstructs the 18 truncated-template exclusions from Sharma ICI offsets and waveform length and invalidates stale fixed-suite caches before

reporting. Unless otherwise stated, analyses use 5 blocked folds over Date  $\times$  Unit  $\times$  IDN blocks. The click-level consensus grid is  $K \in \{12, 16, 20, 24, 32\}$ ; the emergent coda inventory grid is  $K \in \{8, 12, 16, 20, 24, 32\}$ . Coda embeddings are reduced to 64 PCA dimensions where PCA is used, and click per-view embeddings are reduced to 32 PCA dimensions. KMeans uses `n_init=10`, random seed 42, scikit-learn default `max_iter=300`, and tolerance  $10^{-4}$ . Phase A uses the `alphabet_style_pairwise_ami_bh_fdr` protocol with 253 encoder-pair comparisons, 200 AMI null permutations, 100 bootstrap resamples, and FDR threshold  $\alpha = 0.05$ . The Phase A target is pairwise cross-encoder AMI among emergent whole-coda partitions; NMI to published Sharma coda type is a descriptive sanity check only.

*Phase A null construction..* For each encoder pair, encoder A labels are held fixed while encoder B labels are shuffled within Date  $\times$  Unit  $\times$  IDN strata. AMI is recom-

puted, repeated for  $n_{\text{null}} = 200$ , and BH-FDR is applied across all 253 encoder-pair tests. This null median is high because Date/Unit/IDN already carries real structure in this single-population deployment. The null is deliberately conservative: it preserves recording-stratum imbalance and asks what cross-encoder agreement remains beyond that.

*Excluded truncated-template codas.* The 18 excluded zero-indexed coda rows are {82, 119, 121, 829, 830, 1075, 1076, 1186, 1262, 1263, 1264, 1265, 1266, 1270, 1275, 1289, 1341, 1389}. The corresponding one-indexed IDs are {83, 120, 122, 830, 831, 1076, 1077, 1187, 1263, 1264, 1265, 1266, 1267, 1271, 1276, 1290, 1342, 1390}. All 18 are EC1, but the pre-exclusion set is also EC1, so this is not a clan-selective exclusion. By unit, the exclusions are A=3, F=15, D=0. By date, the exclusions are 20/01/2010=3, 03/02/2005=2, 05/05/2008=2, 02/02/2010=1, and 12/02/2010=10. By coda type, 1+1+3 accounts for 12/18, 5-NOISE for 1/18, 10R for 1/18, 6-NOISE for 2/18, and 7D1 for 2/18.

Family	Base checkpoint	Views / notes
AVES	aves-base-bio	aves/mean, aves_L4/mean, aves_L6/mean, aves_L8/mean
AVES2	esp-aves2-sl-beats-base	aves2_L4/mean, aves2_L6/mean, aves2_L8/mean; aves2/mean dropped by curation
HuBERT	facebook/hubert-base	hubert_L0/mean, hubert_L4/mean, hubert_L6/mean, hubert_L8/mean
OpenBEATs/BEATs	beats_iter3+_as2m	openbeats/mean, openbeats_L4/mean, openbeats_L6/mean, openbeats_L8/mean
wav2vec 2.0	facebook/wav2vec2-base	wav2vec2_L4/mean, wav2vec2_L6/mean, wav2vec2_L8/mean; wav2vec2/mean dropped by curation
Whisper	openai/whisper-small	whisper/mean; included in Phase A coda views, excluded from click-level 20-view suite
Perch	perch_v2	perch/mean, perch_32k/mean; perch/mean excluded from click-level 20-view suite, perch_32k/mean retained where eligible
VampNet	default	vampnet/mean, vampnet_32k/mean; vampnet/mean excluded from click-level 20-view suite, vampnet_32k/mean retained where eligible
SoundStream	-	soundstream/mean dropped by curation

**Table B.2**

Encoder-view and checkpoint details. All Phase A / primary view names here are mean pooled. Most paths use fixed-suite 16 kHz inputs; perch\_32k/mean and vampnet\_32k/mean are high-SR/native-rate aliases. Phase A uses the 23 whole-coda views listed above excluding the three globally dropped views. The click-level 20-view suite excludes whisper/mean, perch/mean, and vampnet/mean, while retaining perch\_32k/mean and vampnet\_32k/mean.

Analysis	Eligible views	Eligibility / curation rule
Phase A emergent coda inventory	23 whole-coda views	Uses all curated coda views; 253 encoder-pair comparisons = $\binom{23}{2}$
T1b/T2b/T3b/T8 click-tier tests	20 curated click views	Excludes whisper/mean, perch/mean, and vampnet/mean; retains 32 kHz aliases where eligible
Bridge 6 matched-multiset test	23 coda views	Uses all coda views available for the matched-multiset coda-embedding association test
Phase F click stretch	18 views	perch_32k/mean and vampnet_32k/mean are missing from the aligned per-click stretch arm
Phase F coda stretch	23 views	Uses all coda views available for whole-waveform and ICI-only coda-stretch comparisons

**Table B.3**

Encoder-view eligibility by analysis. The previous ambiguity between 20 and 23 views is resolved here: Phase A used 23 whole-coda views, while the click-level suite uses 20 curated click views.

Test	Tokens / input space	Estimator	Null and key knobs
T1b	Click consensus alphabet	NMI(click multiset, coda label)	Label shuffle on coda labels; cross-block Date $\times$ Unit $\times$ IDN
T2b	Click consensus alphabet	Bigram lift and positional MI	Within-coda click shuffle
T3b	Click consensus alphabet	Class-balanced linear probe; accuracy/macro-F1/top-3	Shuffled-label null; ordered-vs-bag companion
T8	Click consensus alphabet	Context-position Spearman and $R^2$ probe	Previous/own/next vs. own-only and shuffled-target null
Phase A	Emergent whole-coda VQ partitions	Pairwise cross-encoder AMI among partitions; descriptive NMI to Sharma label	Date $\times$ Unit $\times$ IDN-stratified label shuffle; $K \in \{8, 12, 16, 20, 24, 32\}$
Phase C	Exact click-token strings	Reuse fraction	Length-matched multinomial null
Phase E	Coda-token streams	NSB second-order TE and entropy lifts	Within-bout shuffle; 43 bouts / 1,481 codas TE-effective sample
Bridge 6	Matched click-multiset pairs	Spearman $\rho$ (ICI-pattern distance, coda-embedding distance)	9,450 matched pairs from 211 groups; group-aware permutation and group bootstrap

**Table B.4**

Per-test protocol summary. Tokenisation at the click level uses the 20-view consensus alphabet of §3; tokenisation at the coda level uses the same two-stage procedure on per-coda embeddings, with Phase A using 23 views. Blocked CV uses 5 folds over Date  $\times$  Unit  $\times$  IDN blocks. Permutation-based statistics use the stated null construction; Phase E robustness streams are not independent biological samples.